

## Zn-Fe and Zn-Fe-Y Cementation Coatings for Enhancing Corrosion Resistance of Steel

Sirong Yu<sup>\*</sup>, Li Liu

College of Mechanical and Electronic Engineering, China University of Petroleum (East China),  
Qingdao 266580, P.R China

\*E-mail: [liuli1212006@outlook.com](mailto:liuli1212006@outlook.com)

*Received: 22 March 2017 / Accepted: 18 April 2017 / Published: 12 May 2017*

---

This work aims to enhance the corrosion resistance of medium carbon steel 45. Zn-Fe coatings on steel 45 were prepared at different temperatures (380°C, 390°C, 400°C and 410°C) by pack cementation process. The microstructure, formation mechanism and corrosion behavior of the Zn-Fe coatings were investigated. The Zn-Fe coating possessed a two-layered structure consisting of a thin diffusion layer and a thick outer layer. The coating thickness increased with the increase of the temperature. Zn-Fe-Y coating on steel 45 was prepared by the pack cementation process at 390°C. The effect of Y addition on the microstructure and corrosion behavior of the Zn-Fe coating was studied. The structure of the Zn-Fe-Y coating was similar to that of the Zn-Fe coating. The coating thickness increased with the addition of Y. The activation energies for the formation of the Zn-Fe and the Zn-Fe-Y coatings were 82.31 kJ/mol and 81.12 kJ/mol, respectively. The corrosion resistance was measured by the immersion test and polarization test. The results showed that the corrosion resistance of the Zn-Fe coating firstly increased and then decreased with the increase of temperature. The Zn-Fe-Y coating had better corrosion resistance than the Zn-Fe coating.

---

**Keywords:** Coating; Microstructure; Y<sub>2</sub>O<sub>3</sub>; Activation energy; Corrosion resistance.

### 1. INTRODUCTION

Fasteners are the key parts to maintain the normal operation of the ocean platform. Medium carbon steel is commonly used in the manufacture of fasteners because of its high strength, hardness and performance-price ratio [1]. In ocean environment, the medium carbon steel suffers from serious corrosion. The corroded fasteners produce severe effects on the service life and operation security of the ocean platform. Therefore, how to enhance the corrosion resistance of medium carbon steel has getting much attention.

Many surface treatment techniques are effective to enhance the corrosion resistance of steel substrate, such as electroplating, physical vapor deposition (PVD), micro-arc oxidation (MAO), chemical vapor deposition (CVD) and thermal spraying [2-4]. Among various surface treatment techniques, the pack cementation considered as a reaction of chemical vapor deposition is a cost-effective and easy-to-operate technique to enhance the corrosion resistance of steel substrate [5]. Four procedures occur during the pack cementation process [6, 7]. Firstly, metal halide is formed by the reaction of activator with source element. Secondly, the metal halide diffuses from the pack mixture to the substrate driven by concentration gradient. Thirdly, the source element is deposited on the substrate surface through the reduction reaction of the metal halide on the substrate surface. Lastly, the source element continually diffuses into the substrate.

Al has been successfully applied in the pack cementation method [8-9]. Hu et al studied the microstructure of Al coating on 310 stainless steel by the pack cementation at 900°C for 5 h [10]. Hounjiou et al investigated the high temperature oxidation behavior of Al cementation coating on Fe-30Cr alloy [11]. This pack cementation was performed at 1000°C for 5 h. According to the above, the aluminizing method has the disadvantages of high working temperature, dust pollution and material oxidation. Therefore, pack cementation coatings carried out at low temperatures are urgent to be developed.

As it is anodic to Fe and consequently plays a sacrificial anode effect, Zn can be used as a corrosion-resistant coating of steel by electroplating and hot dipping [12, 13]. In recent years the Zn coating prepared by pack cementation at low temperature was developed. The Zn cementation coating has been widely applied in enhancing the corrosion resistance of Mg alloys and copper [7, 14]. At present the research of Zn-Fe cementation coating about enhancing the corrosion resistance of medium carbon steel is not perfect. The effect of heating temperature on the Zn pack cementation coating is little investigated. In this work, Zn-Fe coatings on medium carbon steel 45 were prepared by the pack cementation method at different temperatures (380°C, 390°C, 400°C and 410°C) for 4 h. The effects of heating temperature on the microstructure and corrosion behavior of the Zn-Fe coatings were investigated. The formation process of the coatings was discussed. It was reported that adding trace amounts of rare earth (RE) element could effectively improve the adhesion of coating [15]. There is a great significance to study the microstructure and corrosion behavior of Zn-Fe-RE coating. Zn-Fe-Y coating on medium carbon steel 45 was prepared by pack cementation at 400°C for 4 h. The addition of Y on the microstructure, formation mechanism and corrosion resistance of Zn-Fe coating were analysed.

## 2. EXPERIMENTAL

### 2.1 Preparation of coating

Medium carbon steel 45 used as substrate was cut into specimens with a dimension of 3 mm × 15 mm × 20 mm. The chemical compositions of the medium carbon steel 45 are listed in Table 1. Before the pack process, the specimens were ground by 2000 grid SiC paper, washed with alcohol, and

dried with warm flowing air.

**Table 1.** Chemical compositions of medium carbon steel 45 (wt.%)

C	Si	Mn	P	S	Cr	Ni	Cu	Fe
0.46	0.27	0.64	0.03	0.02	0.02	0.02	0.02	Balance

Zn-Fe and Zn-Fe-Y coatings on medium carbon steel 45 were prepared using the pack cementation process. The pack mixture for the Zn-Fe coating was composed of Zn and  $\text{NH}_4\text{Cl}$  powders. The Zn-Fe-Y coating was prepared by the the addition of  $\text{Y}_2\text{O}_3$  to the pack. The specimen was placed in an  $\text{Al}_2\text{O}_3$  crucible filled with mixed pack. Then the crucible was covered with an  $\text{Al}_2\text{O}_3$  lid, and sealed with high temperature resistant sand. The heating process was performed in a box-type resistance furnace filled with inert gas. The crucible was heated to the desired temperature and held at this temperature for 4 h. Then the crucible was cooled inside the furnace to room temperature. The heating temperature and compositions of the pack mixture are listed in Table 2.

**Table 2.** Temperature and compositions of the pack mixture

Coating	Temperature (°C)	Pack powder (wt.%)		
		$\text{NH}_4\text{Cl}$	$\text{Y}_2\text{O}_3$	Zn
Zn-Fe	380	2	0	Balance
Zn-Fe	390	2	0	Balance
Zn-Fe	400	2	0	Balance
Zn-Fe	410	2	0	Balance
Zn-Fe-Y	400	2	2	Balance

## 2.2. Characterization of coating

The cross-sectional morphologies of coated specimens were observed using optical microscope (OM). The thickness of the coatings was derived from the OM photographs. The phases of the coatings were examined using X-ray diffraction (XRD). The chemical compositions of the Zn-Fe and Zn-Fe-Y coatings were measured with a scanning electron microscopy (SEM) with an energy dispersive spectrometry (EDS).

## 2.3 Corrosion behavior

The corrosion rates of the substrate and different coated specimens were examined by immersion test at room temperature. The specimen was placed in a glass beaker with 200 ml of 3.5 wt.% NaCl solution. The weight change of the specimen was measured every day by an electronic scale with a weighing accuracy of 0.1 mg. After 30 days, the immersion test was terminated and the specimen was taken out. The corrosion rate ( $C_R$ ) was worked out by Eq. (1):

$$C_R = \Delta m / (At) \quad (1)$$

where  $\Delta m$  is the weight change (g),  $A$  is the surface area ( $m^2$ ), and  $t$  is the immersion time (d). The phases of the corrosion products were examined using XRD.

After the immersion test, the potentiodynamic polarization behaviors of the substrate and coated specimens were investigated using the CS350 electrochemical workstation. When the open circuit potential became roughly stable after the specimen immersed into the 3.5 wt.% NaCl solution for 30 minutes, the test began.

### 3. RESULTS AND DISCUSSION

#### 3.1 Coating characterization

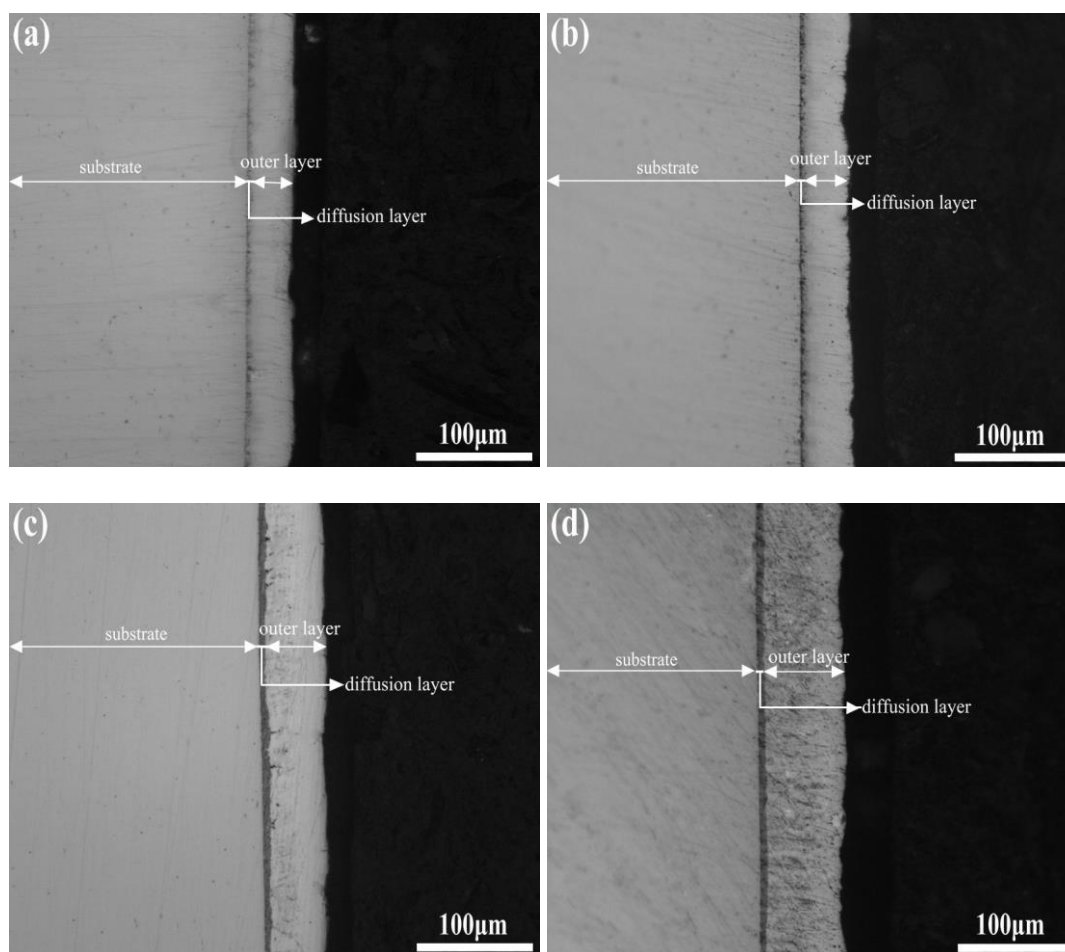


**Figure 1.** Cross-sectional morphologies of Zn-Fe coatings on steel 45 formed at different temperatures (a) 380°C, (b) 390°C, (c) 400°C, (d) 410°C

Fig. 1 shows the cross-sectional morphologies of Zn-Fe coatings formed at different temperatures. The coatings are continuous and having good adhesion with the substrate. The surface of the coatings is ragged. No penetrating cracks and big holes are found in the coatings. The coating thickness always increases with the increase of the temperature. All coatings show a similar two-

layered structure consisting of a thick outer layer and a thin diffusion layer. The similar structure has been reported in other cementation coatings [22]. The uniformity of the thickness increases with the increase of the temperature. Some defects such as tiny fissures are found in the coating formed at 410°C. The quality of the coating firstly increases and then decreases with increasing the temperature. The Zn-Fe coating formed at 400°C shows the best quality.

Fig. 2 shows the relationship between the thickness and the temperature. The thicknesses of the coatings formed at 380°C, 390°C, 400°C and 410°C are 39.2 μm, 43.6 μm, 56.7 μm and 75.9 μm, respectively. The outer layer thicknesses of the four coatings are 38.6 μm, 42.1 μm, 52.0 μm and 69.4 μm in sequence. Both the diffusion zone thickness and the out layer thickness increase rapidly with the increase of the temperature. When the temperature varies from 380°C to 390°C, the thicknesses of the outer layer and the diffusion layer increase a little. They change a lot with further increasing the temperature from 390°C to 410°C.

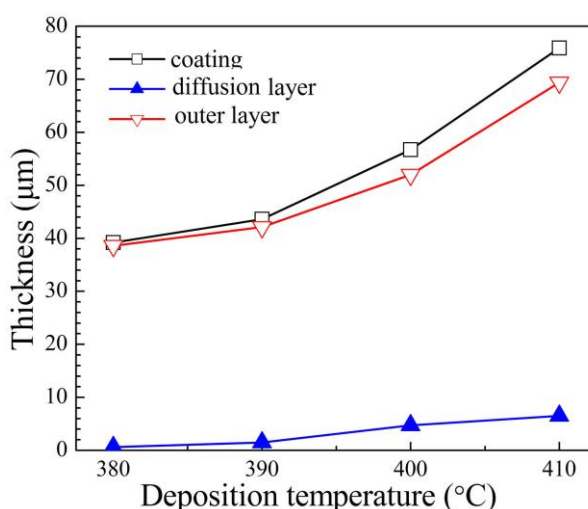


Figure 2. Relationship between the thickness and temperature

Fig. 3 shows the napierian logarithm of the coating thickness varying with the 1/T×1000 (T is the absolute temperature). According to the fitting results, the formation of the Zn-Fe coating is well consonant with the Arrhenius relationship. The relationship between the temperature (T) and coating growth rate (k) can be described using Eq. (2) [16]:

$$\ln k = -\frac{E}{RT} + \ln A \tag{2}$$

where E is the activation energy, R is the gas constant, and A is a constant. According to the Fick's second law [17], the relationship between the coating growth rate and the coating thickness is expressed using Eq. (3):

$$k = \frac{x}{\sqrt{t}} \tag{3}$$

Substituting Eq. (3) into Eq. (2), Eq. (4) is educed:

$$\ln x = -\frac{E}{RT} + \ln A + \ln \sqrt{t} \tag{4}$$

The slope of the fitting straight line is -9.99. By the calculation, the activation energy is 82.31 kJ/mol for the formation of the Zn-Fe coating (Eq. (4)).

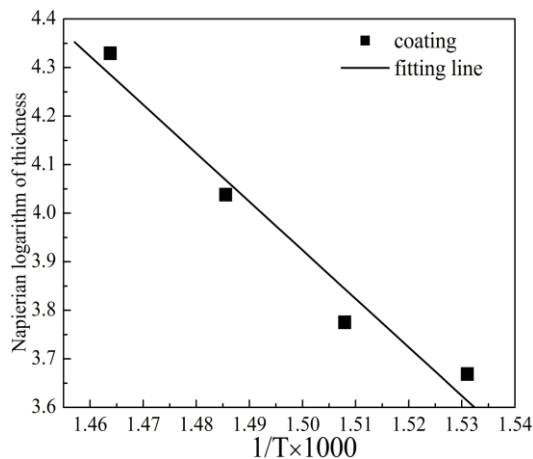


**Figure 3.** Napierian logarithm of thickness of Zn-Fe coating varying with 1/T×1000

Fig. 4 shows the cross-sectional microstructure of the Zn-Fe-Y coating formed at 400°C. The thickness of Zn-Fe-Y coating is 70.1 μm, which is much larger than the Zn-Fe coating formed at 400°C (Fig. 1c). With the addition of Y, the coating thickness has increased by 13.4 μm. The thickness of the outer layer is 66.5 μm, and the thickness of the diffusion layer is 3.6 μm. The thickness of the Zn-Fe-Y coating is more uniform than that of the Zn-Fe coating formed at 400°C. No obvious defects are found in the Zn-Fe-Y coating. The addition of Y<sub>2</sub>O<sub>3</sub> can improve the quality of the coating.

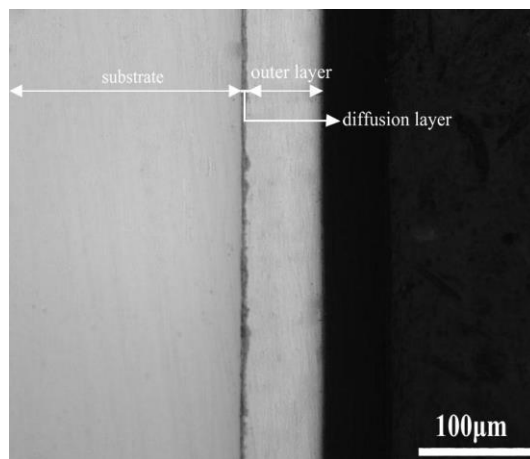


**Figure 4.** Cross-sectional microstructure of Zn-Fe-Y coating on steel 45 formed at 400°C

Fig. 5 shows the cross-sectional SEM graph and element content profile of the Zn-Fe coating formed at 400°C. According to the Fick's first law [18, 19], it is concluded that the formation of the

coatings is due to the inward diffusion of active Zn atoms and the outward diffusion of active Fe atoms. The outer layer contains large amounts of Zn and small amounts of Fe. The content of Zn in the outer layer decreases slowly from the coating's surface to the substrate. The diffusion layer is composed of large amounts of Fe and small amounts of Zn. The Zn concentration of the diffusion zone decreases sharply from the outside to the inside. A small amount of Zn atoms have diffused into the substrate. According to previous studies [20], the formation of the Zn-Fe coating is controlled by vacancy diffusion.

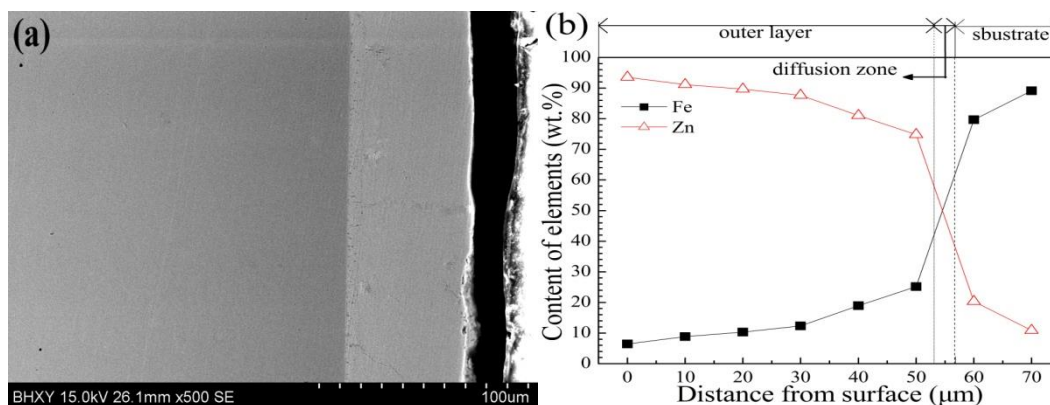


**Figure 5.** Cross-sectional SEM graph (a) and element content profile (b) of the Zn-Fe coating formed at 400°C

Before the specimen was heated, Zn atoms were in direct contact with Fe atoms. A number of vacancies existed in the substrate surface. After the specimen was heated, the active Zn atoms were formed through the following chemical reaction equations:



The concentration of active Zn atoms in the pack were higher than that on the substrate surface. The inward diffusion of Zn was owing to the concentration gradient between the pack and the substrate surface. The active Zn atoms easily diffused into the substrate along the vacancies, which could result in the serious lattice distortion of the substrate. Fe atoms in the substrate surface were activated through the following reaction equations:



The serious lattice distortion accelerated the outward diffusion of active Fe atoms.

Fig. 6 shows the SEM graph and element content profile of the Zn-Fe-Y coating formed at 400°C. The coating is mainly composed of large amounts of Zn, small amounts of Fe, and trace amounts of Y. The content of Fe in the Zn-Fe-Y coating was obviously larger than that in the Zn-Fe coating. More Zn atoms have diffused into the substrate. It is obvious that the addition of Y can accelerate the inward diffusion of active Zn atoms and the outward diffusion of active Fe atoms. This

accelerating effect is ascribed to the active Y atoms. The active Y atoms formed through the following reaction equations:



The accelerating effect of the active Y atoms is explained as follow. The active Y atoms with high chemical reactivity and low electronegativity have a high affinity with none metallic elements [21]. Thus, the Y atoms can remove the contaminants in the substrate surface, which promotes the adsorption of Zn atoms on the substrate surface. The Y atoms can be easily adsorbed on the surface of the steel substrate due to its high surface activity [22], providing the channels for the diffusion of Zn atoms. Comparing Fig 4b and Fig. 4d, the concentration of Zn atoms in the substrate increased with the addition of Y. The possible reason is as follows. Once the amount of the active Y atoms on the substrate surface reaches a proper value, the Y atoms can diffuse into the interior of the steel along the crystal defects such as crystal boundaries and dislocations [23]. The severe lattice distortion increases with the inward diffusion of Y atoms with large radius, which provides the channels for the inward diffusion of Zn atoms.

Substituting Eq. (2) into Eq. (3), Eq. (12) is obtained:

$$E = RT(\ln A - \ln x + \ln \sqrt{t}) \tag{12}$$

According to Eq. (12), the relationship between the two coating thicknesses can be expressed in the following equations:

$$\ln x_2 - \ln x_1 = \frac{E_1 - E_2}{RT} \tag{13}$$

$$E_1 - E_2 = RT \ln \frac{x_2}{x_1} \tag{14}$$

$$E_2 = E_1 - RT \ln \frac{x_2}{x_1} \tag{15}$$

The activation energy is 81.12 kJ/mol for the formation of the Zn-Fe-Y coating. With the addition of  $\text{Y}_2\text{O}_3$ , the activation energy decreased.

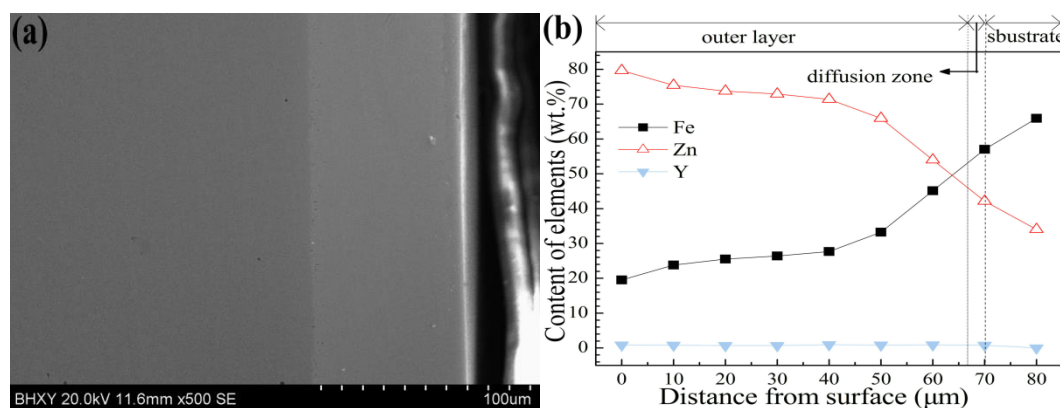


**Figure 6.** Cross-sectional SEM graph (a) and element content profile (b) of the Zn-Fe-Y coating formed at 400°C

Fig. 7 gives the phases of the Zn-Fe and Zn-Fe-Y coatings formed at 400°C. The Zn-Fe coating is composed of  $\text{FeZn}_9$  and  $\text{Fe}_{11}\text{Zn}_{40}$  phases, which confirmed that the formation of the Zn-Fe coating is attributed to the inward diffusion of Zn and the outward diffusion of Fe.  $\text{YZn}_5$  phase was formed with the addition of  $\text{Y}_2\text{O}_3$ , which proves that the Y participated in the formation of the coating.

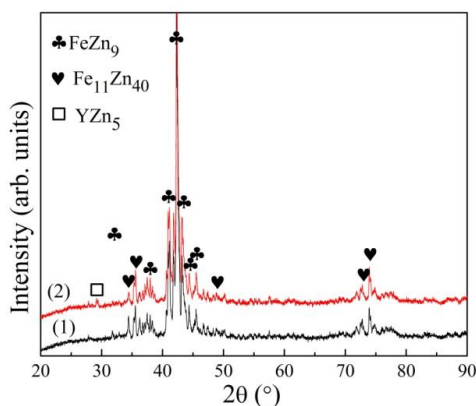


**Figure 7.** Phases of coatings formed at 400°C (1) Zn-Fe coating, (2) Zn-Fe-Y coating

### 3.2 Corrosion resistance

After the immersion test, the corrosion morphology of each specimen was observed. Fig. 8 shows the corrosion morphologies of the substrate and different coated specimens. The substrate has been seriously corroded. Dark brown and yellow rusts are observed on the surface. The rusts of loose structure are easy to break off, which can not prevent the penetration of  $\text{Cl}^-$ . For the Zn-Fe coating formed at 380°C, most of the coating surface is covered with white particles. The rest of the coating surface still keeps its original grey color. The similar corrosion morphology was reported in the Zn coating prepared by thermal spraying [23]. The Zn-Fe coatings formed at 390°C and 400°C shows a similar corrosion morphologies to the Zn-Fe coating formed at 380°C except for the particle sizes. The higher the temperature, the smaller the particles are. From the corrosion morphologies, it is difficult to determine which one of the Zn-Fe coatings formed at 390°C and 400°C shows better corrosion resistance. For the Zn-Fe coating formed at 410°C, a white powder layer almost covers the entire surface. Small white sheets are slightly observed at the edge of the coating. Many slightly larger white particles are unevenly distributed on the powder layer. It is clear that the Zn-Fe coating formed at 410°C exhibits worse corrosion resistance than other Zn-Fe coatings. For the Zn-Fe-Y coating, almost no serious corrosion can be seen. Only a small portion of the surface is covered with white powders. It is obtained that the addition of Y can improve the corrosion resistance of Zn-Fe coating.

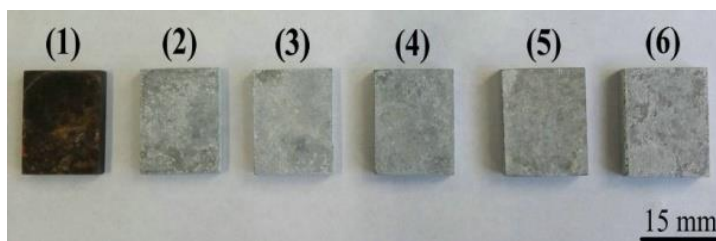


**Figure 8.** Corrosion morphologies of substrate and different coated specimens (1) substrate, (2) Zn-Fe coating, 380°C, (3) Zn-Fe coating, 390°C, (4) Zn-Fe coating, 400°C, (5) Zn-Fe-Y coating, 400°C, (6) Zn-Fe coating, 410°C

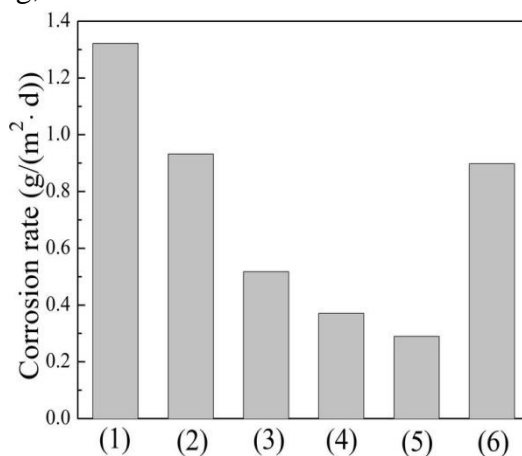


**Figure 9.** Corrosion rates of substrate and different coatings (1) substrate, (2) Zn-Fe coating, 380°C, (3) Zn-Fe coating, 390°C, (4) Zn-Fe coating, 400°C, (5) Zn-Fe-Y coating, 400°C, (6) Zn-Fe coating, 410°C

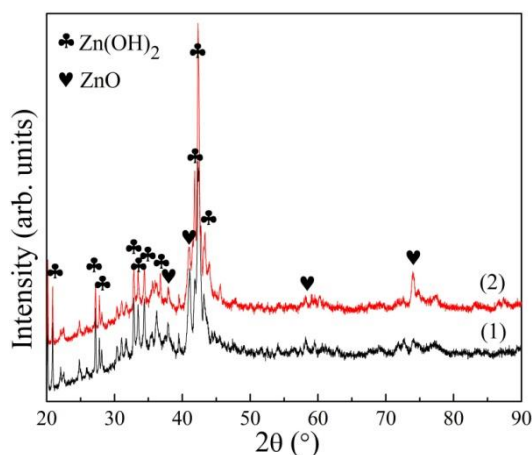


**Figure 10.** Phases of corrosion products on different coatings formed at 400°C (1) Zn-Fe coating, (2) Zn-Fe-Y coating

Fig. 9 shows the corrosion rates of different specimens. The corrosion rate of the substrate is 1.322 g/(m<sup>2</sup>·d). The corrosion rates of the Zn-Fe coatings formed at 380°C, 390°C, 400°C and 410°C are 0.932 g/(m<sup>2</sup>·d), 0.571 g/(m<sup>2</sup>·d), 0.371 g/(m<sup>2</sup>·d) and 0.898 g/(m<sup>2</sup>·d), respectively. It is clear that the Zn-Fe coatings play an active role in the protection of the substrate. With the increase of the temperature, the corrosion resistance of the Zn-Fe coating firstly increases and then decreases. The

similar result has been reported in other coatings [24, 25]. The Zn-Fe coating formed at 400°C shows the best corrosion resistance. The corrosion rate of the Zn-Fe-Y coating is 0.290 g/(m<sup>2</sup>·d). It can be found that the corrosion resistance of Zn-Fe-Y coating is better than that of the Zn-Fe coating. There are two reasons for the improving corrosion resistance with Y addition. Firstly, the Y in the coating can promote the formation of a continuous and dense ZnO scale through the third element effect of Y [26, 27]. The third element Y could lower the amount of Zn needed for protective ZnO scale formation. Thus, the formation of a protective ZnO film is accelerated. Secondly, this improvement of corrosion resistance is due to the formation of YZn<sub>5</sub> phase. The phase containing Y can enhance the stability of the corrosion product film on the coating surface [28], thus the corrosion damage was retarded. The similar effect of rare earth element has been reported in other pack cementation coatings [29]. Fig. 10 shows the phases of the corrosion products. The corrosion products are composed of ZnO and Zn(OH)<sub>2</sub>, which confirms that Zn played a sacrificial anode role during the immersion process, and the corrosion of the substrate was prevented.

Fig. 11 shows the polarization curves of different specimens. Table 3 gives the corrosion potential ( $E_{\text{corr}}$ ), corrosion current density ( $i_{\text{corr}}$ ), cathodic Tafel slope ( $\beta_c$ ), anodic Tafel slope ( $\beta_a$ ) and polarization resistance ( $R_p$ ) based the polarization curves.  $R_p$  was worked out by Eq. (16) [30]:

$$R_p = \frac{\beta_a \beta_c}{2.303 i_{\text{corr}} (\beta_a + \beta_c)} \quad (16)$$

The  $E_{\text{corr}}$  of the coated specimen shifts to the negative value, which is due to the fact that the potential of Zn (-0.76 V) is lower than that of Fe (-0.44 V). The  $E_{\text{corr}}$  of Zn-Fe coating formed at 400°C is higher than that of the Zn-Fe coatings formed at 380°C, 390°C and 410°C. The  $i_{\text{corr}}$  value of each coated specimen is much smaller than that of the substrate. Namely, the corrosion resistance of the coated specimen is better than that of the substrate. Therefore, the Zn-Fe coating plays a sacrificial anode role in the corrosion process, and the substrate is effectively protected. The  $\beta_a$  of the substrate is larger than that of the coated specimens. The  $\beta_a$  of the Zn-Fe-Y coating is lower than that of the Zn-Fe coatings, which implies that the corrosion products film on Zn-Fe-Y coating provides better protection. The  $i_{\text{corr}}$  value of the Zn-Fe coating increases to the maximum and then decreases with increasing heating temperature. The Zn-Fe coating formed at 400°C gives the smallest  $i_{\text{corr}}$  value, which suggests that the Zn-Fe coating formed at 400°C exhibits the best corrosion resistance than other Zn-Fe coatings. The  $E_{\text{corr}}$  shifts towards the positive direction with the addition of Y in the pack. The  $i_{\text{corr}}$  of the Zn-Fe-Y coating is smaller than that of the Zn-Fe coating, which suggests that the corrosion resistance of the Zn-Fe-Y coating is better than that of the Zn-Fe coating. The  $R_p$  of the substrate is lower than that of the coated specimens, which shows that the substrate shows the worst corrosion resistance. For the Zn-Fe coatings, the coating formed at 400°C exhibits the largest  $R_p$  value. The  $R_p$  value of the Zn-Fe-Y coatings is larger than that of the Zn-Fe coatings. The result of the polarization test agrees well with that of the immersion test.

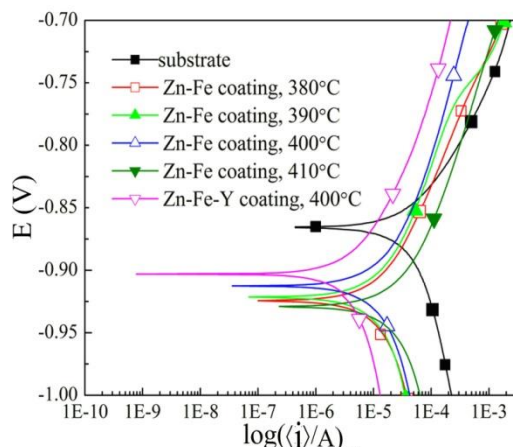


Figure 11. Polarization curves of substrate and different coatings

Table 3. Corrosion potential, corrosion current density, cathodic Tafel slope, anodic Tafel slope and polarization resistance revealed by the polarization curves

Specimen	$E_{corr}$ (V)	$i_{corr}$ (mA/cm <sup>2</sup> )	$\beta_c$ (mV)	$\beta_a$ (mV)	$R_p$ ( $\Omega \cdot cm^2$ )
substrate	-0.865	$3.25 \times 10^{-3}$	49.35	62.58	$3.69 \times 10^3$
Zn-Fe coating, 380°C	-0.925	$3.21 \times 10^{-4}$	45.78	60.93	$3.54 \times 10^4$
Zn-Fe coating, 390°C	-0.921	$3.30 \times 10^{-4}$	48.55	60.69	$3.55 \times 10^4$
Zn-Fe coating, 400°C	-0.912	$2.19 \times 10^{-4}$	43.70	45.72	$4.43 \times 10^4$
Zn-Fe coating, 410°C	-0.931	$2.86 \times 10^{-4}$	45.06	43.72	$3.34 \times 10^4$
Zn-Fe-Y coating, 400°C	-0.901	$1.78 \times 10^{-4}$	42.01	41.05	$5.06 \times 10^4$

#### 4. CONCLUSIONS

(1) The Zn-Fe coatings on medium carbon steel 45 were successfully obtained by pack cementation at 380°C, 390°C, 400°C and 410°C. With the increase of the temperature, the coating thickness gradually increased. The activation energy was 82.31 kJ/mol for the formation of the Zn-Fe coating. The coatings possessed a two-layered structure of a thick outer layer and a thin diffusion layer.

(2) The Zn-Fe-Y coating on steel 45 was successfully obtained by the pack cementation at 400°C. The Zn-Fe-Y coating has a similar structure to the Zn-Fe coating. The addition of Y significantly increased the coating thickness. The activation energy was 81.12 kJ/mol for the formation of the Zn-Fe-Y coating.

(3) The Zn-Fe and Zn-Fe-Y coatings both played an active role in protecting the substrate. With increasing temperature, the corrosion resistance of the Zn-Fe coating increased to the maximum and then decreased. The Zn-Fe coating formed at 400°C exhibited the best corrosion resistance.

(4) The addition of Y into the Zn-Fe coating could enhance the corrosion resistance.

## ACKNOWLEDGEMENT

This work was supported by the Fundamental Research Funds for the Central Universities (16CX06020A).

## References

1. A. Kuduzović, M.C. Poletti, C. Sommitsch, M. Domankova, S. Mitsche and R. Kienreich, *Mater. Sci. Eng., A*, 590 (2014) 66.
2. S. Ghaziof and W. Gao, *Appl. Surf. Sci.*, 351 (2015) 869.
3. M. Hashempour, A. Vincenzo, F. Zhao and M. Bestetti, *Mater. Charact.*, 92 (2014) 64.
4. A. Kumar, A. Sharma and S.K. Goel, *Appl. Surf. Sci.*, 370 (2016) 418.
5. Z.D. Xiang, J.S. Burnell-Gray and P.K. Datta, *J. Mater. Sci.*, 36 (2001) 5673.
6. Z. Zhan, Y. He, D. Wang and W. Gao, *Intermetallics*, 14(2006): 75.
7. G. Hu, Z. Xu, J. Liu and Y. Li, *Surf. Coat. Technol.*, 203 (2009) 3392.
8. F. Bozza, G. Bolelli, C. Giolli, A. Giorgetti, L. Lusvarghi, P. Sassatelli, A. Scrivani, A. Candeli and M. Thoma, *Surf. Coat. Technol.*, 239 (2014) 147.
9. N. Vialas and D. Monceau, *Surf. Coat. Technol.*, 201(2006) 3846.
10. K.G. Anthymidis, N. Maragoudakis, G. Stergioudis, O. Haidar and D.N. Tsipas, *Mater. Lett.*, 57 (2003) 2399.
11. C. Houngiou, S. Chevalier and J. P. Larpin, *Oxid. Met.*, 65 (2006) 409.
12. A.R. Marder, *Prog. Mater. Sci.*, 45 (2000) 191.
13. N. Pistofidis, G. Vourlias, D. Chaliampalias, K. Chrysafis, G. Stergioudis and E. K. Polychroniadis, *J. Alloys Compd.*, 407(2006) 221.
14. H. Wang, B. Yu, W. Wang, G. Ren, W. Liang and J. Zhang, *J. Alloys Compd.*, 582 (2014) 457.
15. R. Thanneeru, S. Patil, S. Deshpande and S. Seal, *Acta Mater.*, 55 (2007) 3457.
16. M. Qiao and C. Zhou, *Surf. Coat. Technol.*, 206 (2012) 2899.
17. D. Stathokostopoulos, D. Chaliampalias, E.C. Stefanaki, G. Polymeris, E. Pavlidou, K. Chrissafis, E. Hatzikraniotis, K.M. Paraskevopoulos and G. Vourlias, *Appl. Surf. Sci.*, 285 (2013) 417.
18. Z.D. Xiang and P.K. Datta, *Mater. Sci. Eng., A*, 356 (2003) 136.
19. Z.D. Xiang and P.K. Datta, *Surf. Coat. Technol.*, 184 (2004): 108.
20. M.F. Yan, *Mater. Chem. Phys.*, 70 (2001) 242.
21. Y.S. Tian, C.Z. Chen, L.X. Chen and Q.H. Huo, *Scripta Mater.*, 54 (2006) 847.
22. X. Zhao and C. Zhou, *Corros. Sci.*, 86 (2014) 223.
23. H. Katayama and S. Kuroda, *Corros. Sci.*, 76 (2013) 35.
24. R. Sako and J. Sakai, *Surf. Coat. Technol.*, 219 (2013) 42.
25. H. Elentriecy, H. Luo, H. Meyer, L. Grado and J. Qu, *Electrochim. Acta.*, 123 (2014) 58.
26. Y. Niu, X.J. Zhang, Y. Wu and F. Gesmundo, *Corros. Sci.*, 48 (2006) 4020.
27. T.J. Luo, Y.S. Yang, Y.J. Li and X.G. Dong, *Electrochim. Acta.*, 54 (2009) 6433.
28. G. Wu, Y. Fan, H. Gao, C. Zhai and Y. Zhu, *Mater. Sci. Eng., A*, 408 (2005) 255.
29. N. Lin, F. Xie, T. Zhong, X. Wu and W. Tian, *J. Rare. Earth.*, 28 (2010) 301.
30. F. Wei, W. Zhang, T. Zhang and F. Wang, *Int. J. Electrochem. Sci.*, 12 (2017) 155.